nature geoscience

LETTERS

PUBLISHED ONLINE: 17 OCTOBER 2010 | DOI: 10.1038/NGEO979

Northern Hemisphere atmospheric stilling partly attributed to an increase in surface roughness

Robert Vautard[1]*, Julien Cattiaux[1], Pascal Yiou[1], Jean-Noël Thépaut[2] and Philippe Ciais[1]

Surface winds have declined in China, the Netherlands, the Czech Republic, the United States and Australia over the past few decades[1–4]. The precise cause of the stilling is uncertain. Here, we analyse the extent and potential cause of changes in surface wind speeds over the northern mid-latitudes between 1979 and 2008, using data from 822 surface weather stations. We show that surface wind speeds have declined by 5–15% over almost all continental areas in the northern mid-latitudes, and that strong winds have slowed faster than weak winds. In contrast, upper-air winds calculated from sea-level pressure gradients, and winds from weather reanalyses, exhibited no such trend. Changes in atmospheric circulation that are captured by reanalysis data explain 10–50% of the surface wind slowdown. In addition, mesoscale model simulations suggest that an increase in surface roughness—the magnitude of which is estimated from increases in biomass and land-use change in Eurasia—could explain between 25 and 60% of the stilling. Moreover, regions of pronounced stilling generally coincided with regions where biomass has increased over the past 30 years, supporting the role of vegetation increases in wind slowdown.

The decline of surface wind observed in many regions of the world is a potential concern for wind power electricity production[5], and has been shown to be the main cause of decreasing pan evaporation[6–8]. In China, a persistent decrease of monsoon winds was observed in all seasons[3,9]. Stilling winds were also evidenced over the Netherlands[2], in the Czech Republic[10], over the conterminous US (refs 1,11) and most of Australia[4]. In Mediterranean regions, wind trends were non-monotonic over the past decades[12]. At high latitudes, the surface winds were found to increase[13,14].

Such surface wind trends can be due to (1) changes in mean circulation[15,16] and/or to the decrease of synoptic weather system intensity, both as a consequence of climate change, (2) changes in near-surface wind due to increasing surface roughness in the near field of each station[2,4,11] and/or in boundary layer structure, and/or (3) instrumental or observational drifts[17,18]. Over China, wind decline was attributed to a north–south warming gradient in winter, and to sunlight dimming caused by air pollution lingering over central areas[3,9] in summer. No clear explanation was given for the wind decline in other studied regions of interest.

The attribution of the stilling drivers requires a global investigation of available surface and upper-air wind data, which has not been conducted so far. Here we use global data sets of *in situ* wind measurements (see the Methods section and Supplementary Information). A set of 822 worldwide surface stations with continuous wind records was selected after careful elimination of stations with obvious breaks and large gaps. This data set covers most of the northern mid-latitudes over the 1979–2008 period.

We found that annual mean wind speeds have declined at 73% of surface stations over the past 30 years (Fig. 1a). In Europe, Central Asia, Eastern Asia and in North America (Fig. 1a) the annual mean surface wind speed has decreased on average at a rate of -0.09, -0.16, -0.12 and $-0.07\,\mathrm{m\,s^{-1}}$ decade^{-1}, respectively (-2.9, -5.9, -4.2 and -1.8% per decade), that is, a decrease of about 10% in 30 years and up to almost 20% in Central Asia, where wind speed trends have not been studied so far. These numbers are all statistically significant ($p < 0.1\%$ for the regression coefficient). Tropical areas are not well covered by the data set. However the wind decline over South Asia is also about -5% per decade, and $-0.08\,\mathrm{m\,s^{-1}}$ per decade.

Zonal means of wind trends exhibit a rather homogeneous behaviour across latitudes, in the range of -0.06 to -0.11 to $\mathrm{m\,s^{-1}}$ decade^{-1}. A higher frequency of positive trends is found only over the ∼15 northern polar latitude stations. A few wind series starting earlier (after 1959) further indicate that stilling actually started at least as early as in the 1960s (Supplementary Fig. S1). Negative trends were also found in mid to high percentiles of the wind speed distribution (see Supplementary Table S1), as well as in the frequency of observations above fixed mid to high thresholds (5–15 $\mathrm{m\,s^{-1}}$, see Fig. 2). Trend results are robust to changes in the station selection method and parameters (see Supplementary Table S1).

If we assume that the primary cause of the surface wind stilling is a slowdown in atmospheric general circulation and/or a weakening in synoptic weather activity, then a stilling trend should also show up (1) in the reanalyses of three-dimensional wind fields of the National Centers for Environmental Prediction/National Center of Atmospheric Research (NCEP/NCAR) and European Center for Medium-range Weather Forecast (ECMWF)—because observations of upper-air winds are used in the reanalysis procedure and there is a high connectivity between winds at 10 m and at 850 hPa, see Supplementary Fig. S2, (2) in upper-air wind observations from rawinsonde and (3) in geostrophic winds deduced from pressure gradients.

NCEP/NCAR reanalysis[19] does not exhibit any trend in surface (10 m) winds over land (Fig. 1b), as found in previous studies[2,4,11]. The recent ECMWF ERA-interim reanalysis[20] exhibits negative trends with magnitudes between 10% (for North America) and 50% (for Europe) of the observed ones over the past two decades, with quite different spatial patterns (Fig. 1c, Supplementary Fig. S1 and Table S1). Over Australia similar weak trends ($-0.02\,\mathrm{m\,s^{-1}}$ decade^{-1}) were obtained by ERA-interim as by ERA40 in a previous study[4]. In contrast the inter-annual variability of surface winds is fairly well reproduced in both reanalyses (Supplementary Figs S2 and S3). This indicates that part of the wind trend changes, captured in the ERA-interim reanalyses, is due to large-scale circulation changes, but the reanalysis

[1]LSCE/IPSL, Laboratoire CEA/CNRS/UVSQ, 91191 Gif/Yvette Cedex, France, [2]ECMWF, Shinfield Park, Reading RG2 9AX, UK.
*e-mail: robert.vautard@lsce.ipsl.fr.

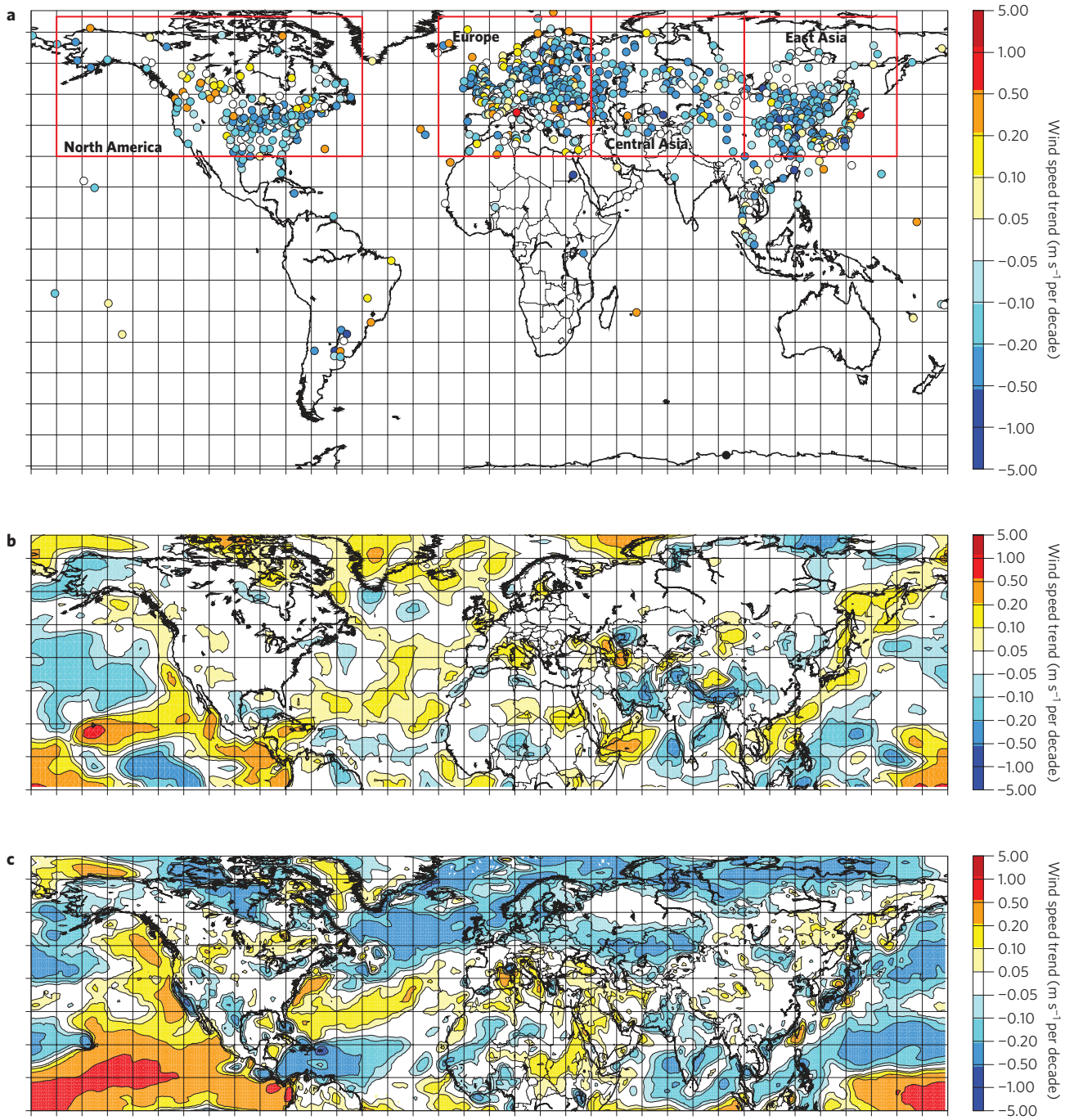

Figure 1 | Observed and reanalysis surface wind speed trends. a, 30-year surface (1979–2008) wind speed linear trend calculated over all of the available observations and each of the selected stations, in m s^{-1} per decade. The specific regions studied in this Letter are shown by rectangles delimiting the areas over which statistics are calculated. **b**, NCEP/NCAR reanalyses trends calculated using mean daily 10 m wind speed values available over a grid of 193 × 47 grid points over the Northern Hemisphere (data available at http://www.cdc.noaa.gov/data/gridded/data.ncep.reanalysis.html). **c**, The same as in **b** for ERA-interim reanalyses trends calculated over the past 20 years alone. The area boundaries for the four regions of focus are: Europe 20° W–40° E, 30°–75 N, 276 stations; Central Asia 40°–100° E, 30°–75° N, 96 stations; Eastern Asia 100°–160° E, 30°–75° N, 190 stations; North America, 170°–50° W, 30°–75° N, 170 stations. The South Asia area quoted in the main text covers 40°–160° E, 0°–30° N, 40 stations.

models/procedures have deficiencies and/or missing key processes that prevent the surface wind trends from being fully resolved[2,4,11]. Land-use changes, not taken into account in reanalyses, are potential candidates of such processes.

Upper-air (850 hPa and above) wind speed observations from rawinsonde data do not either exhibit such a systematic wind decline pattern (Fig. 3), and even show large regions with increasing trends (Western Europe, North America). At nearly collocated sites, winds normalized by their grand mean have trends with much higher amplitudes at the surface than above (Fig. 3c). However, regionally coherent negative trends are found over Eastern Asia at 850 hPa, where surface trends could be linked with upper-air trends, as a result of regional monsoon decline due to climate change and air pollution[3]. However, reanalyses over China do not exhibit trends, which remains unexplained and points towards uncertainties in models.

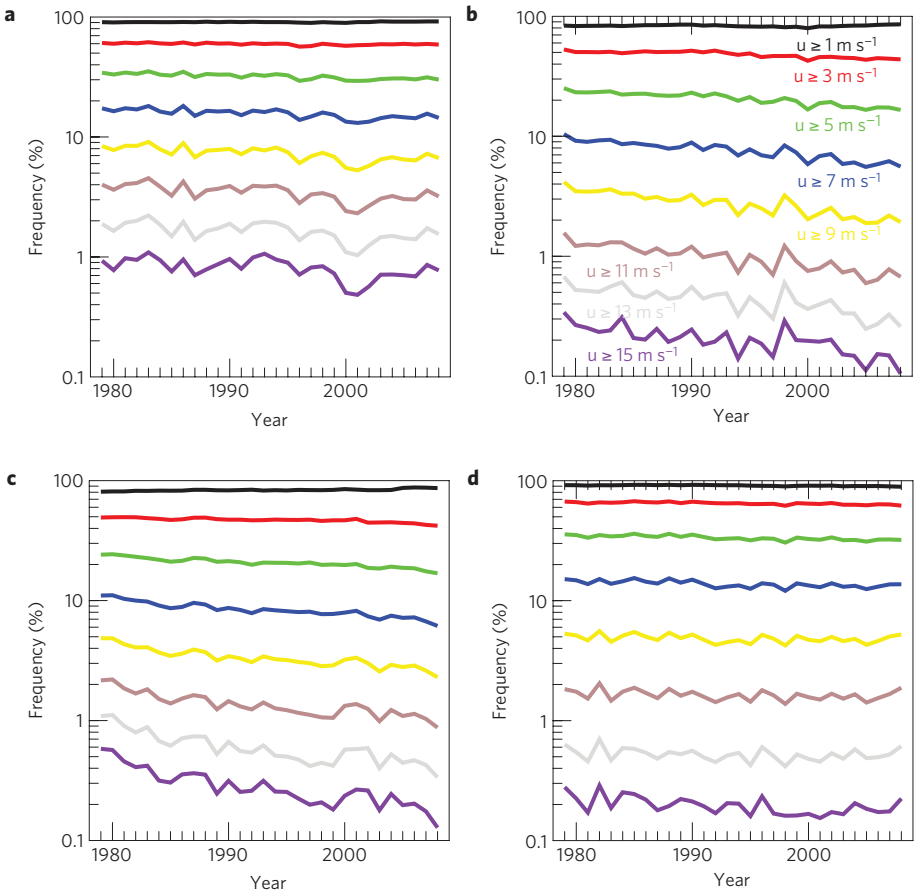

Figure 2 | Wind speed distribution evolution. a–d, Evolution, as a function of year, of the annual frequency of wind exceeding a given threshold (various curves, see legend), for each of the four regions identified in Fig. 1: Europe (**a**), Central Asia (**b**), Eastern Asia (**c**), North America (**d**). The numbers take into account all stations in the domains together, as well as all hours and seasons. The linear regression trend coefficients, respectively for the frequency (in % per decade) of winds stronger than 1, 3, 5, 7, 9, 11, 13 and 15 m s^{-1} are: Europe: 0, −1, −5, −7, −11, −12, −11, −12; Central Asia: 0, −6, −13, −18, −23, −24, −22, −23; Eastern Asia: 2, −4, −10, −15, −19, −23, −30, −37; Northern America: −1, −2, −4, −5, −3, −3, −3, −11.

Geostrophic winds estimated from observed sea-level pressure gradients also show a negligible stilling trend[2,8] (Supplementary Fig. S3). However, their interannual variations are consistent with observed surface winds. These findings suggest that large-scale wind changes should not be the dominant drivers of observed surface wind decline.

Despite our stringent station selection procedure of rejecting stations with large data gaps and obvious breaks (see the Methods section and Supplementary Information), some time series may still exhibit heterogeneities, which could explain a widespread wind stilling trend only if they would be coherent over all regions, which is unlikely. Systematical instrumental drifts, such as anemometer performance degradation, especially for near-calm winds, have been suggested[17], but anemometers were replaced over the past decades (O. Mestre and S. Jourdain, Météo-France, personal communication), and trends are more pronounced for stronger winds. A systematic change of observation systems or round-off procedures[18] also could have introduced artificial trends. However, at most stations the decreasing wind trend was gradual throughout the past 30 years, as shown for instance in Fig. 4a for the Central Asian stations with wind trends in the lowest tercile of the data. It is therefore unlikely that generalized instrumental heterogeneities and observational procedures explain the systematic trends.

These findings suggest that changes in surface processes could play a major role in the surface wind stilling. Surface winds are sensitive to changes in (1) surface roughness and (2) sensible heat fluxes modifying vertical momentum fluxes through boundary layer convection. Wind trends do not exhibit strong diurnal variations (see Supplementary Table S1), suggesting that roughness changes should dominate over sensible heat flux changes as a cause of stilling.

Increase of surface roughness can be associated with factors such as urbanization, growth of forests, changes in trees and forest distribution or changes in agricultural practices. To estimate the sensitivity of surface wind to roughness changes, we carried out sensitivity simulations with the MM5 model[21]. Starting from a control simulation (with standard roughness height z_{0c}), changes in roughness height z_0 (from a factor 1 to 2) have been applied in the model surface boundary conditions during a single year (2007) over an area covering Eastern Europe and Central Asia, where the negative wind trends are most pronounced. When averaged over the area considered (Supplementary Fig. S4), the 10 m wind speed decrease δU between an enhanced roughness simulation and a control simulation fits the relation $\delta U = -a\ln(z_0/z_{0c})$, where $a = 0.48$ m s^{-1} when surface roughness is uniformly changed and $a = 0.37$ m s^{-1} when only grassland roughness is changed and the effect is averaged over grassland areas (as defined by MM5 land-cover data). Thus, about a doubling of roughness height would lead to a decrease of 10 m wind by 0.26–0.33 m s^{-1}, which is in the range of observed wind decreases over the past three decades (see Supplementary Table S1). Over Central Asia, where trends are most pronounced, a tripling of the roughness height would be required to fully reach observed stilling, which seems fairly unrealistic.

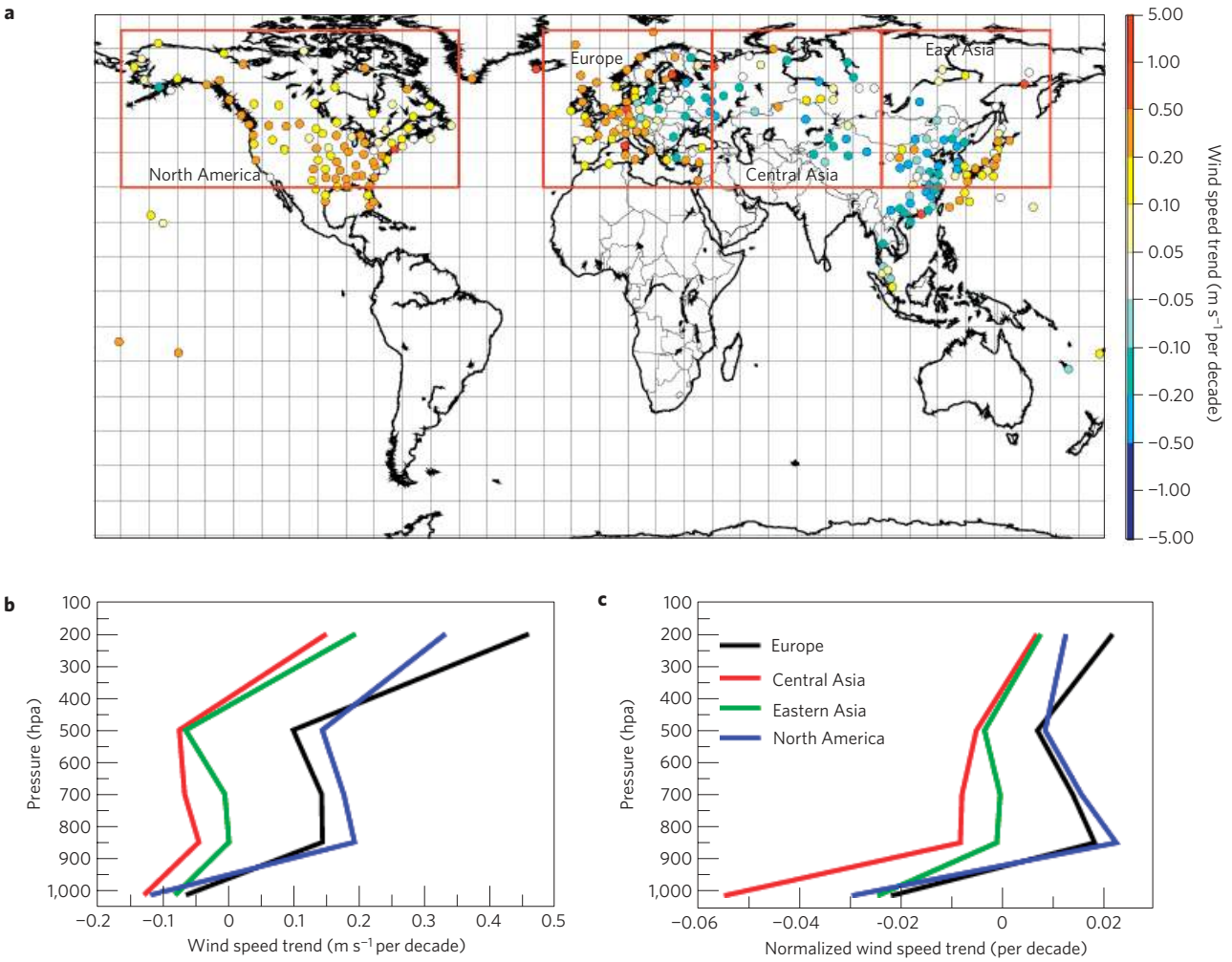

Figure 3 | Upper-air wind speed trends. a, Trends of the 850 hPa wind measured by rawinsonde data, over stations having at least half of the yearly data over more than 15 years during the two-decade period between 1979 and 2008, in m s^{-1} per decade. **b**, Mean vertical profile of wind speed trend obtained from monthly averaged rawinsonde measurements (850 hPa and above) and closest surface site, averaged over all sites in each region of Fig. 1a. **c**, The same as in **b** for wind speed trends normalized by mean wind speed at each site. Surface values are arbitrarily set to 1,015 hPa pressure in the profile.

An average increase of about 1.1% per year of forest carbon sink at mid to high latitudes of the Northern Hemisphere band has been deduced from two-decade-long remote-sensed normalized difference vegetation index (NDVI) data[22]. Over Russia, estimates of the yearly carbon sink to carbon pool ratio vary between 1.2 and 1.3%. Using a theory developed to link tree properties and roughness[23,24], applied to areas with only sparse roughness elements (which is generally the case for anemometer neighbourhoods), the roughness height should scale as $z_0 \sim h\lambda^{1.33}$, where h is the height and λ is the frontal area index of roughness elements. Assuming an isotropic development of the volume V of roughness elements and their constant density per area, h scales as $V^{1/3}$ and λ scales as $V^{2/3}$, implying that z_0 scales as $V^{1.22}$. Conversely, assuming only an increase in the density of roughness elements without any change in their volume, the increase of z_0 should scale as the increase of V. From this scaling one can deduce that the increase of biomass over Russia would have induced, over 30 years, an increase of roughness height of 36–50%, explaining 25–40% of the observed wind stilling. This is also supported by the cropland abandonment in southwestern Russia[25]. The contribution of biomass growth to wind stilling should be higher in other areas such as Europe or China, where forest growth reaches 1.5% per year (refs 26,27). In such cases, the induced wind decline could reach between 40% and 60% of the observed one over the past three decades.

Several studies based on the NDVI showed a widespread increase of vegetation in many northern areas[28]. Using the Global Inventory Modelling and Mapping Studies (GIMMS) database[29], obtained from the Advanced Very High Resolution Radiometer (AVHRR) remote-sensed observations over 1982–2006, we found that 62% of wind sites witnessed a positive spring–summer NDVI trend (Fig. 4b). Moreover, the negative wind trend has a median amplitude about three times larger over sites with a NDVI trend in the upper 10% than over sites in the lower 10% of its distribution (Fig. 4c). This also supports the influence of vegetation increase on surface winds, but a quantitative relationship between NDVI and roughness is difficult to establish. Note also that the declining wind trends are found across the entire day (Supplementary Table S1), suggesting that dynamic roughness changes dominate over sensible heat flux changes.

Therefore, atmospheric circulation changes captured by the ERA-interim reanalysis explain between 10 and 50% of wind stilling in the northern mid-latitudes, and our analysis suggests that 25–60% could be due to a roughness increase due to vegetation. Urbanization may be an extra roughness increase factor, although recent observations do not directly support this mechanism[8]. However, even a gross estimate of roughness increase due to urbanization could not be found. To formally attribute the causes of declining winds, a sensitivity analysis

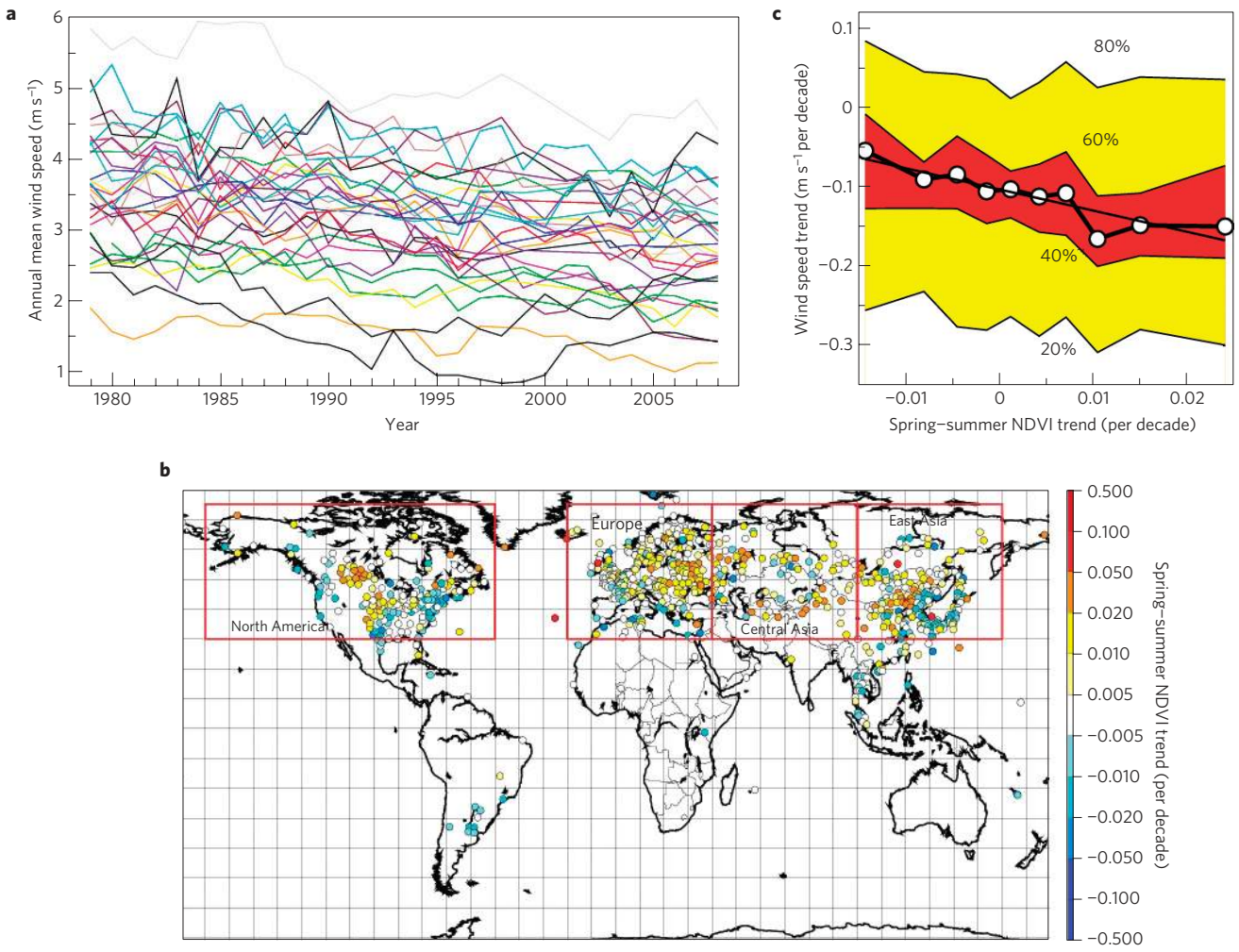

Figure 4 | Surface wind trends and their relationship with NDVI trends. a, Time evolution of annual average surface wind speed for each of the stations with the trend in the lower tercile of the wind trend distribution over the Central Asia area. Each curve corresponds to a station. The mean trend is $-0.31\,m\,s^{-1}$ decade^{-1}. **b**, Spring–Summer (April–September) trends (in decade^{-1}), of the average over a 24×24 km area around the surface wind stations of the NDVI (as obtained from the GIMMS AVHRR product). **c**, Median surface wind trends over the stations of each decile of the NDVI trend distribution, together with the corresponding wind trend distribution (20–40% and 60–80% in yellow, 40–60% in red), versus the median of each decile of NDVI trends. The regression line for the median ($y = -0.104 - 2.65x$) is shown.

using a model of surface wind speeds driven by all potential variables is required.

An important question is whether wind power energy production is likely to be affected by wind stilling in the future. Over the past 30 years surface winds underwent an average 10% decrease, with larger trends at stronger winds (Fig. 2). As wind electricity production is much more efficient at stronger winds, a continuation of such trends would lead to a major loss of wind power production. However, wind power is not taken at the surface but between 50 and 100 m, where trends should be weaker according to our three-dimensional analysis. In any case, the strong influence of land-cover change on wind speed trends is good news because land use can much more easily be controlled locally than the large-scale circulation.

Methods

Surface winds. Observation data sets come from the Research Data Archive, which is maintained by the Computational and Information Systems Laboratory at NCAR (sponsored by the National Science Foundation). The original data were taken from the Research Data Archive (http://dss.ucar.edu).

Surface winds are obtained from two global data sets of this archive, gathering hourly or three-hourly meteorological information on several parameters including wind speed and direction from anemometers. The first data set (DS463.2) covers the period 1901–2003. The second data set (DS461.0) covers the period 2000–2008. Both contain hourly or three-hourly reports from about 10,000 observation sites worldwide. The database includes data originating from various sources such as synoptic, airways, Meteorological Routine Weather Report and Supplementary Marine Reporting Station. A full description of the data sets can be found on the websites http://dss.ucar.edu/datasets/ds463.2/docs/td9956.200301.pdf and http://dss.ucar.edu/datasets/ds461.0/docs/. In particular, care was taken to correct some heterogeneities induced by changes in wind speed units in this data set (see related documentation on this latter website).

A stringent objective procedure is applied here to remove stations with gaps or heterogeneities in the data, as described in the Supplementary Information, leaving a subset of 822 worldwide stations, most of which are located in the Northern Hemisphere.

Upper-air winds from rawinsondes. We used the rawinsonde monthly averages of wind gathered in the Integrated Global Radiosonde Archive[30] (IGRA). These data were available for comparison with surface data over the three-decade period from 1979 to 2008, and we used values taken at standard levels of 850 hPa, 700 hPa, 500 hPa and 200 hPa. A site selection procedure is also applied as for surface data, see Supplementary Information. IGRA also includes surface wind speed taken near the site. However, we did not use these data because the pairing would have led to less complete profiles than if using the NCAR surface wind data and a criterion of 300 km for distance. We however checked that the IGRA surface wind speed had similar trends to the NCAR data.

NCEP/NCAR and ERA-interim reanalyses. Reanalyses issued at NCEP/NCAR are used, and made available at a $2.5 \times 2.5°$ resolution on the

http://www.cdc.noaa.gov/data/gridded/data.ncep.reanalysis.html website. Only the 4 × daily data set of wind at 10 m is used, for the Northern Hemisphere over the period 1979–2008. The new ECMWF ERA-interim[20] is a global atmospheric reanalysis covering the period from 1989 until real time. The production of ERA-interim began in summer 2006. Increased computer power enabled several enhancements of ERA-interim over ERA-40. In particular, ERA-interim uses a model version that was operational for weather forecast in the autumn of 2006, with improved model physics. It also uses a 12-h 4D-VAR data assimilation system, a horizontal resolution of ~80 km, a more extensive use and better treatment of satellite radiances, a better formulation of background error constraints and a new humidity analysis. The long-term homogeneity has improved substantially over that of ERA-40. The reader is referred to http://www.ecmwf.int/research/era/do/get/index for a description of reanalysis activities and products at ECMWF.

NDVI from AVHRR. NDVI data from the GIMMS database[29], obtained from the AVHRR remote-sensed observations, were used. These data cover the 25-year period 1982–2006 and were carefully calibrated. They were originally provided on a 8 km × 8 km grid, but averages over available NDVI data over the nine cells surrounding the station were used for plotting Fig. 4b,c. We then calculated linear trends from six-month NDVI averages (April–September).

Received 22 April 2010; accepted 9 September 2010; published online 17 October 2010

References

1. Klink, K. Trends in monthly maximum and minimum surface wind speeds in the coterminous United States, 1961 to 1990. *Clim. Res.* **13,** 193–205 (1999).
2. Smits, A., Klein-Tank, A. M. G. & Können, G. P. Trends in storminess over the Netherlands, 1962–2002. *Int. J. Climatol.* **25,** 1331–1344 (2005).
3. Xu, M. *et al*. Steady decline of East Asian monsoon winds, 1961–2000: Evidence from direct measurements of wind speed. *J. Geophys. Res.* **111** doi:10.1029/2006JD007337 (2006).
4. McVicar, T. R. *et al*. Wind speed climatology and trends for Australia, 1975–2006: Capturing the stilling phenomenon and comparison with near-surface reanalysis output. *Geophys. Res. Lett.* **35** doi:10.1029/2008GL035627 (2008).
5. Pryor, S. C., Barthelemie, R. J. & Schoof, J. T. Interannual variability of wind indices across Europe. *Wind Energy* **9,** 27–38 (2005).
6. Roderick, M. L., Rotstayn, L. D., Farquhar, G. D. & Hobbins, M. T. On the attribution of changing pan evaporation. *Geophys. Res. Lett.* **34,** L17403 (2007).
7. Roderick, M. L., Hobbins, M. T. & Farquhar, G. D. Pan evaporation trends and the terrestrial water balance II. Energy balance and interpretation. *Geogr. Compass* **3,** 761–780 (2009).
8. Rayner, D. P. Wind run changes: The dominant factor affecting pan evaporation trends in Australia. *J. Clim.* **20,** 3379–3394 (2007).
9. Hua, G., Ming, X. & Qi, H. Changes in near-surface wind speed in China: 1969–2005. *Int. J. Climatol.* **30** doi:10.1002/joc.2091 (2010).
10. Brazdil, R. *et al*. Climate fluctuations in the Czech Republic during the period 1961–2005. *Int. J. Climatol.* **29,** 223–242 (2009).
11. Pryor, S. C. *et al*. Wind speed trends over the contiguous United States. *J. Geophys. Res.* **114,** D14105 (2009).
12. Pirazzoli, P. A. & Tomasin, A. Recent near-surface wind changes in the Central Mediterranean and Adriatic areas. *Int. J. Climatol.* **23,** 963–973 (2003).
13. Aristidi, E. *et al*. An analysis of temperatures and wind speeds above Dome C, Antarctica. *Astron. Astrophys.* **430,** 739–746 (2005).
14. Lynch, A. H., Curry, J. A., Brunner, R. D. & Maslanik, J. A. Toward an integrated assessment of the impacts of extreme wind events on Barrow, Alaska. *Bull. Am. Meteorol. Soc.* **85,** 209–221 (2004).
15. Lu, J., Vecchi, G. A. & Reichler, T. Expansion of the Hadley cell under global warming. *Geophys. Res. Lett.* **34,** L06805 (2007).
16. Seidel, D. J., Fu, Q., Randel, W. J. & Reichler, T. J. Widening of the tropical belt in a changing climate. *Nature Geosci.* **1,** 21–24 (2008).
17. DeGaetano, A. T. Identification and implications of biases in US surface wind observation, archival, and summarization methods. *Theor. Appl. Climatol.* **60,** 151–162 (1998).
18. McKee, T. B., Doesken, N. J., Davey, C. A. & Pielke, R. A. Climate data continuity with ASOS: Report for period April 1996 through June 2000, 82, Colo. Clim. Cent., Fort Collins (2000).
19. Kalnay, E. *et al*. The NCEP/NCAR 40-year reanalysis project. *Bull. Am. Meteorol. Soc.* **77,** 437–471 (1996).
20. Uppala, S., Dee, D., Kobayashi, S., Berrisford, P. & Simmons, A. Towards a climate data assimilation system: Status update of ERA-Interim. *ECMWF Newslett.* **115,** 12–18 (2008) (Available at: http://www.ecmwf.int/publications/newsletters/).
21. Dudhia, J. A nonhydrostatic version of the Penn State/NCAR mesoscale model: Validation tests and simulation of an Atlantic cyclone and cold front. *Mon. Weath. Rev.* **121,** 1493–1513 (1993).
22. Myneni, R. B. *et al*. A large carbon sink in the woody biomass of Northern forests. *Proc. Natl Acad. Sci.* **98,** 14784–14789 (2001).
23. Raupach, M. R. Drag and drag partition on rough surfaces. *Bound. Layer Meteorol.* **60,** 375–395 (1992).
24. Raupach, M. R. Simplified expressions for vegetation roughness length and zero-plane displacement as a function of canopy height and area index. *Bound. Layer Meteorol.* **71,** 211–216 (1994).
25. Vuichard, N. *et al*. Carbon sequestration due to the abandonment of agriculture in the former USSR since 1990. *Glob. Biogeochem. Cycles* **22,** GB4018 (2008).
26. Ciais, P. *et al*. Carbon accumulation in European forests. *Nature Geosci.* **1,** 425–429 (2008).
27. Kauppi, P. E. *et al*. Returning forests analysed with the forest identity. *Proc. Natl Acad. Sci.* **103,** 17574–17579 (2006).
28. Donohue, R. J., McVicar, T. R. & Roderick, M. L. Climate-related changes in Australian vegetation cover as inferred from satellite observations for 1981–2006. *Glob. Change Biol.* **15,** 1025–1039 (2009).
29. Tucker, C. J. *et al*. An extended AVHRR 8-km NDVI data set compatible with MODIS and SPOT vegetation NDVI data. *Int. J. Remote Sens.* **26,** 4485–5598 (2005).
30. Durre, I., Russell, S., Vose, & Wuertz, D. B. Overview of the integrated global radiosonde archive. *J. Clim.* **19,** 53–68 (2006).

Acknowledgements

We thank X. Wang for his help with extraction of NDVI fields at the stations. We benefited from fruitful discussions with F-M. Bréon at LSCE.

Author contributions

R.V. designed the experiments and carried out the observation analysis, J.C. did all model experiments and analysis of outputs, as well as NCEP/NCAR reanalysis calculations. J-N.T. extracted and analysed all data from ERA-interim reanalyses. P.Y. initially suggested systematic wind trends in observations, and P.C. suggested that land-cover changes due to vegetation could be a major driver of wind stilling and helped design the experiments with NDVI. All co-authors substantially contributed to the paper writing.

Additional information

The authors declare no competing financial interests. Supplementary information accompanies this paper on www.nature.com/naturegeoscience. Reprints and permissions information is available online at http://npg.nature.com/reprintsandpermissions. Correspondence and requests for materials should be addressed to R.V.